

## THE IMPACT OF SIZE-DEPENDENT PREDATION ON POPULATION DYNAMICS AND INDIVIDUAL LIFE HISTORY

DAVID CLAESSEN,<sup>1,2,3</sup> CATELIJNE VAN OSS,<sup>1</sup> ANDRÉ M. DE ROOS,<sup>1</sup> AND LENNART PERSSON<sup>2</sup>

<sup>1</sup>*Institute for Biodiversity and Ecosystem Dynamics, Section Population Biology, University of Amsterdam, P.O. Box 94084, 1090 GB Amsterdam, The Netherlands*

<sup>2</sup>*Department of Ecology and Environmental Science, Aquatic Ecology Group, Umeå University, S-901 87 Umeå, Sweden*

**Abstract.** In size-structured predator–prey systems, capture success depends on the sizes of both predator and prey. We study the population-dynamic consequences of size-dependent predation using a model of a size-structured, cannibalistic fish population with one shared, alternative resource. We assume that a prey can be captured by a predator if the ratio of prey length to predator length is within a specific range, referred to as the “predation window.” We find that the lower limit of the predation window ( $\delta$ ) has a major impact on population dynamics, whereas the upper limit ( $\varepsilon$ ) mainly affects population structure and individual life history. For large  $\delta$ , cannibalism cannot decimate young-of-year (YOY) cohorts. Size-dependent competition then results in recruit-driven, single-cohort cycles. With low  $\delta$ , cannibalism regulates recruitment, resulting in coexistence of many year classes. With intermediate  $\delta$ , periods of regulation by cannibalism alternate with periods with severe competition. Occasional high densities of small individuals enable a few cannibals to reach giant sizes, producing a bimodal population size distribution. With small  $\varepsilon$ , all individuals remain small; the population is stunted. Large piscivores can exist only if induced dynamically in population fluctuations. Above a critical  $\varepsilon$ , large piscivores are present permanently, even in stable populations. The critical effect of  $\varepsilon$  relates to the ontogenetic niche shift from planktivory to piscivory. Observed population dynamics of Eurasian perch, yellow perch, and Arctic char, described in the literature, are discussed and, based on our modeling results, can be related to differences in the predation windows of these species. We argue that the effects of  $\delta$  and  $\varepsilon$  relate to two fundamentally different and mutually exclusive aspects of cannibalism.

**Key words:** Arctic char; competition; Eurasian perch; life history, individual; physiologically structured population model; piscivory; population dynamics; predation, size dependent; predator size relative to prey size; size-dependent cannibalism; yellow perch.

### INTRODUCTION

The ability of a predator to capture, kill, and handle prey depends on both predator size and prey size in many species (Wilbur 1988, Shine 1991, Sousa 1993, Triplet and Perrin 1994, Hirvonen and Ranta 1996, Mittelbach and Persson 1998). This is especially evident in cannibalism, where even the roles of predator and prey are often determined by the (relative) sizes of interacting individuals (Fox 1975, Polis 1981, Orr et al. 1990, Fagan and Odell 1996, Dong and DeAngelis 1998, Persson et al. 2000). The minimum prey size a predator can take has been attributed to the predator's ability to detect (Lovrich and Sainte-Marie 1997, Lundvall et al. 1999) or retain (Persson 1987) its prey. Several mechanisms may explain the maximum prey size a predator can take, such as the predator's gape size relative to prey body depth (Werner 1974, Nilsson and Brönmark 2000), or the relative speed of predator and

prey (Christensen 1996). In a review of size-dependent piscivory among diverse fish species, Mittelbach and Persson (1998) show that both the mean, maximum, and minimum sizes of captured fish prey increase with predator size. They found that, across species, the maximum prey length ranged between 35% and 70% of the predator's length, and the minimum between 5% and 25% (see also Lundvall et al. 1999, Persson et al. 2000). Within species, the maximum and minimum prey sizes scale roughly linearly with predator length, so that the ratio of prey length to predator length is a good predictor of predation success. We refer to the range of prey sizes that a predator of a given size can take as its “predation window.”

The predation window is an important link between processes at the individual level and at the population level. It connects prey mortality with the predator size distribution and predator growth rate with the size distribution of prey (Wilbur 1988, Rice et al. 1997). The predation window is therefore likely to have consequences for both individual life history and population dynamics. Life-history consequences may result from the effect of the predation window on the age and size at ontogenetic niche shift (Mittelbach and Persson

Manuscript received 30 January 2001; revised 6 July 2001; accepted 23 July 2001.

<sup>3</sup> Present address: Biomathematics Unit, IACR-Rothamsted, Harpenden AL5 2JQ UK.  
E-mail: david.claessen@bbsrc.ac.uk

1998). Most piscivorous fish have to pass through an invertebrate-feeding stage before entering the piscivorous stage. The size at which a predator can enter the piscivory niche depends on the size scaling of the upper limit of the predation window and the availability of prey sizes. Population-dynamic consequences may result from the effect of the predation window on prey mortality and predator growth. Such effects may, in turn, influence other density- and size-dependent interactions between predator and prey, such as competition (Claessen et al. 2000).

Modeling studies of intraspecific competition in size-structured populations have shown that the dynamics of such populations depend critically on the strength of intercohort competition and how competitive ability changes with body size (Persson et al. 1998). Due to ontogenetic scalings of metabolic and foraging rates, smaller individuals can often sustain themselves at lower resource levels than larger ones, and are hence competitively superior (Persson et al. 1998, Hjelm and Persson 2001). This physiological relationship typically induces population cycles in which abundant recruits control the resource density, and outcompete adult cohorts (Persson et al. 1998). With intraspecific predation, however, adults can decimate the recruit density and hence reduce intercohort competition. By this mechanism cannibalism can dampen population cycles (Claessen et al. 2000). Obviously, this is possible only if newborns are within the predation window of adults. The relation between the lower limit of the predation window, size at reproduction, and size at birth will thus influence whether cannibalism has the potential to regulate population dynamics.

Modeling studies have further shown that the dynamic interplay between size-dependent competition and cannibalism may result in the emergence of size dimorphism, with giant cannibals and dwarf-sized non-cannibals coexisting in a single population (Claessen et al. 2000). The dimorphism is induced by a transition from a phase with weak competition to a phase with strong competition. Before the transition cannibalism by the adult size class decimates the recruits and the absence of intercohort competition allows a range of juvenile and adult sizes to coexist. The transition to severe intra- and intercohort competition occurs when cannibalism fails to control recruitment. Competition for the primary resource causes retarded growth of the recruits and starvation of larger individuals. Of the larger individuals, only those having the recruits within their predation window can switch to cannibalism and survive. By feeding on the slowly growing, dwarf-sized recruits these individuals reach giant sizes. Evidence for giant growth of cannibals induced by population dynamics is found in Eurasian perch (*Perca fluviatilis*) (LeCren 1992, Claessen et al. 2000, Persson et al. 2000).

Giant cannibals are also observed in single-species Arctic char (*Salvelinus alpinus* L.) populations (Parker

and Johnson 1991, Griffiths 1994, Hammar 2000). In contrast with the perch populations, however, it has been claimed that in Arctic char populations giant cannibals are not the result of population fluctuations but rather occur permanently in a stable population size distribution (Parker and Johnson 1991, Johnson 1994). This contrasts with our previous modeling study of size-dependent cannibalism, which predicted that giants and a bimodal population size structure are inherently associated with population fluctuations (Claessen et al. 2000). Explanations of the observed population structure of Arctic char have included ecological factors like cannibalism and parasitism (Hammar 2000), as well as evolutionary factors such as trophic specialization (Parker and Johnson 1991). One of the goals of this present study was to investigate whether both dynamically induced giants, permanent giants, and bimodality can be explained as consequences of size-structured population dynamics, without assuming individual specialization such as learning or flexible behavior. We investigate whether the different patterns can be explained as population-dynamic consequences of different species-specific scalings of the predation window.

We explore the implications of the predation window for population dynamics with a physiologically structured population model of a cannibalistic fish population and its primary, zooplankton resource, developed in Claessen et al. (2000). We determine how the expected type of population dynamics depends on the minimum and maximum prey sizes taken. Based on our previous results (Persson et al. 1998, Claessen et al. 2000), we expect that the lower limit of the predation window determines the ability of cannibals to control recruitment. It may hence affect population dynamics by modifying the scope for intercohort competition. Since the induction of giants by population fluctuations also relates to the ability of cannibals to control recruitment, we expect that the minimum prey size influences the existence of giant cannibals as well. Because, in a stable population, the size at which an individual can enter the piscivory niche depends on the maximum prey size it can take, we investigate how the existence of permanent, large piscivores in stable populations depends on the upper limit of the predation window. We aim to apply our results by linking differences in observed population dynamics between several piscivorous fish species to differences in their predation windows.

## MODEL AND METHODS

### *The model*

Our population-dynamic model of cannibalistic Eurasian perch (*Perca fluviatilis* L.) and its primary, zooplankton resource, is built within the modeling framework of physiologically structured population models (Metz and Diekmann 1986, de Roos 1997). Such mod-

TABLE 1. The model, together with definitions of the state variables and specification of their dynamics.

A) State variables	
Population level	
Number of cohorts, $k$	
Density of cohort $i$ , $N_i$ (no. individuals/L), where $i \in \{1, k\}$	
Individual level	
Irreversible mass, $x_i$ (g)	
Reversible mass, $y_i$ (g)	
Environmental	
Resource density, $R$ (no. individuals/L)	
B) Specification of dynamics	
Within-year dynamics	
Cohort mortality†	$\frac{dN_i}{dt} = -\mu(x_i, y_i)N_i \quad i \in \{1, k\}$
Cohort per capita growth in $x$	$\frac{dx_i}{dt} = \begin{cases} f(x_i, y_i)E_g(x_i, y_i) & \text{if } E_g > 0 \\ 0 & \text{otherwise} \end{cases} \quad i \in \{1, k\}$
Cohort per capita growth in $y$	$\frac{dy_i}{dt} = \begin{cases} (1 - f(x_i, y_i))E_g(x_i, y_i) & \text{if } E_g > 0 \\ E_g & \text{otherwise} \end{cases} \quad i \in \{1, k\}$
Resource dynamics	$\frac{dR}{dt} = r(K - R) - R \sum_{j=1}^k \frac{A_z(x_j)N_j}{1 + H(x_j)\eta(x_j)}$
Between-years: reproduction	
Add one cohort	$k \rightarrow k + 1$
Newborn density	$N_k = \sum_{i=1}^{k-1} F(x_i, y_i)N_i$
Reset adults' mass‡	$y_i = q_i x_i, \quad i \in \{1, k - 1\} \text{ if } F(x_i, y_i) > 0$

Note: The functions defining mortality ( $\mu$ ), energy balance ( $E_g$ ), allocation ( $f$ ), fecundity ( $F$ ), attack rate on zooplankton ( $A_z$ ), handling time ( $H$ ), and encounter rate ( $\eta$ ) are listed in Table 2.

† Cohorts with a density below a trivial threshold (e.g.,  $N = 10^{-12}$  individuals/L) are considered extinct.

‡ Where  $q_i$  = the maximum ratio of non-reproductive, reversible mass to irreversible mass.

els involve state variables at the individual level and the population level (Table 1). The core of our model is an individual-level model of perch that describes the dynamics of the physiological state of individuals depending on the current state and the condition of their environment. The environment consists of the resource population, but also includes the structured population itself, representing all potential cannibals and victims. The state of the population is defined as the distribution of the individuals over all possible individual states. The dynamics of the population are calculated by adding and subtracting the demographic actions (birth, death, growth) of the individuals. In our model we keep track of cohorts of individuals, rather than individuals separately. The dynamics of the state variables in our model are specified in Table 1. Table 2 lists the equations that define the individual-level model. The model parameters, valid for Eurasian perch, are given in Table 3.

Considering the pulsed nature of reproduction in Eurasian perch, we assume in our model that continuous-time growing seasons are alternated by discrete

steps from autumn to spring, in which individuals possibly reproduce (Table 1). We assume that a growing season, in which individuals feed, grow, starve, and possibly die, lasts 90 d, as it does in Central Sweden. We assume that biological activity is negligible outside the growing season, and take the state of the system at the time of reproduction at the start of a growing season identical to that at the end of the previous one. Our model is described in full detail in Claessen et al. (2000), and a closely related model was presented in Persson et al. (1998), where more details on the population-level formulation can be found. Here we restrict our description to the biological assumptions of the model, and focus on two aspects that are of central importance for this article: the predation window and individual growth and starvation.

In our model the physiological state of an individual is characterized by its body mass, which we divide in two state variables: irreversible mass  $x$  and reversible mass  $y$  (Table 1). Reversible mass can be starved away when maintenance requirements exceed the energy in-

TABLE 2. Individual-level functions and their units, representing cannibalistic perch. Only the subscripts  $i$  and  $j$  refer to the cohort index.

Body length, $L$ (mm)	$L = \lambda_1 x^{\lambda_2}$
Zooplankton attack rate, $A_z$ (L/d)	$A_z(x) = \hat{A} \left[ \frac{x}{x_{opt}} \exp \left( 1 - \frac{x}{x_{opt}} \right) \right]^\alpha$
Cannibalistic attack rate, $A_c$ (L/d)	$A_c(c, v) = \begin{cases} \beta c^\sigma \frac{v - \delta c}{(\varphi - \delta)c} & \text{if } \delta c < v \leq \varphi c \\ \beta c^\sigma \frac{\varepsilon c - v}{(\varepsilon - \varphi)c} & \text{if } \varphi c < v < \varepsilon c \\ 0 & \text{otherwise} \end{cases}$
Food intake rate, $I$ (g/d)	$I(x) = \frac{\eta(x)}{1 + H(x)\eta(x)}$
Digestion time, $H$ (d)	$H(x) = \xi_1 x^{\xi_2}$
Total encounter rate, $\eta$ (g/d)	$\eta(x) = \eta_z(x) + \eta_c(x)$
Zooplankton encounter, $\eta_z$ (g/d)	$\eta_z(x) = A_z(x)Rm$
Cannibalistic encounter, $\eta_c$ (g/d)	$\eta_c(x_i) = \sum_j A_c(c_i, v_j)(x_j + y_j)N_j$
Energy balance, $E_g$ (g/d)	$E_g(x, y) = E_a(x) - E_m(x, y)$
Acquired energy, $E_a$ (g/d)	$E_a(x) = k_e I(x)$
Maintenance requirements, $E_m$ (g/d)	$E_m(x, y) = \rho_1(x + y)^{\rho_2}$
Fraction allocated to $x$ , $f$ (g/d)	$f(x, y) = \begin{cases} \frac{1}{(1 + q_1)q_1} \frac{y}{x} & \text{if } x < x_f \\ \frac{1}{(1 + q_A)q_A} \frac{y}{x} & \text{otherwise} \end{cases}$
Fecundity, $F$ (no.)	$F(x, y) = \begin{cases} \frac{e_r(y - q_j x)}{x_b(1 + q_j)} & \text{if } x > x_f \text{ and } y > q_j x \\ 0 & \text{otherwise} \end{cases}$
Total mortality, $\mu$ (d <sup>-</sup> )	$\mu(x, y) = \mu_0 + \mu_s(x, y) + \mu_c(x)$
Starvation mortality, $\mu_s$ (d <sup>-</sup> )	$\mu_s(x, y) = \begin{cases} s(q_s x/y - 1) & \text{if } y < q_s x \\ 0 & \text{otherwise} \end{cases}$
Cannibalistic mortality, $\mu_c$ (d <sup>-</sup> )	$\mu_c(x_j) = \sum_i \frac{A_c(c_i, v_j)N_i}{1 + H(x_i)\eta(x_i)}$

Note: For definitions of  $q_A$ ,  $q_j$ , and  $q_s$ , see Table 3;  $e_r$  = reproductive efficiency;  $k_e$  = intake coefficient (where “e” denotes “energy”).

take rate whereas irreversible mass cannot. Individuals are assumed to be born with a fixed amount of irreversible mass  $x_b$ , and the maximum amount of reversible mass for that size,  $y = q_j x_b$  (Table 3). The ratio of reversible mass over irreversible mass ( $y/x$ ) is assumed to be a measure of the condition of an individual. Body length ( $L$ ) is assumed to depend on irreversible mass alone (Table 2).

All functions of individuals are assumed to depend on their body mass. Attack rates on both zooplankton prey ( $A_z$ ) and conspecific prey ( $A_c$ ) are assumed to depend on irreversible mass only, as empirical data show that they relate strongly to body length (Byström and García-Berthou 1999, Persson et al. 2000, Wahlström et al. 2000). The attack rate on zooplankton is modeled as a dome-shaped curve, reaching a maximum at the optimal size  $x_{opt}$  (Persson et al. 2000, Claessen

et al. 2000). The feeding rate ( $I$ ) is assumed to be limited by the encounter rate with prey mass and the capacity to digest prey mass. We assume that the mass-encounter rate ( $\eta$ ) equals the product of the consumer’s attack rate, prey density, and prey mass. Limitation by digestion capacity is assumed to result in a Holling type II functional response, in which the “handling time” corresponds to the digestion time per gram of prey mass ( $H$ ). The digestion capacity is assumed to increase with irreversible body mass, unaffected by the condition of the individual. The energy intake rate ( $E_a$ ) is found by multiplying the feeding rate with a constant, prey-type independent conversion efficiency,  $k_e$ . We assume “production allocation” (as opposed to assimilation allocation, see Gurney and Nisbet [1998]) of the acquired energy, which means that the acquired energy is used to cover metabolic needs ( $E_m$ ) first, after which

TABLE 3. Model variables and parameters valid for Eurasian perch (*Perca fluviatilis*) feeding on a zooplankton resource (*Daphnia* sp., length 1 mm) and conspecifics.

Subject	Parameter or variable	Value†	Units	Interpretation
Season	$Y$	90	d	length of year
Ontogeny	$x_b$	0.001	g	irreversible mass at birth
	$x_f$	4.6	g	irreversible mass at maturation
	$q_j$	0.74	...	juvenile maximum condition
	$q_A$	1.37	...	adult maximum condition
	$e_r$	0.5	...	gonad-offspring conversion
Length-mass relation	$\lambda_1$	57.6	mm/g $^{\lambda_2}$	allometric scalar
	$\lambda_2$	0.317	...	allometric exponent
Planktivory	$\alpha$	0.62	...	allometric exponent
	$\hat{A}$	$3 \times 10^4$	L/d	max attack rate
	$x_{opt}$	4.7	g	optimal forager size
Piscivory	$\sigma$	0.6	...	allometric exponent
	$\beta$	varied (200)	L·d $^{-1}$ ·mm $^{-\sigma}$	cannibalistic voracity
	$\delta$	varied (0.06)	...	lower limit of predation window
	$\varepsilon$	varied (0.45)	...	upper limit of predation window
	$\phi$	varied (0.2)	...	optimum of predation window
Digestion	$\xi_1$	5.0	d/g $^{(1 + \xi_2)}$	allometric scalar
	$\xi_2$	-0.8	...	allometric exponent
Metabolism	$\rho_1$	0.033	g $^{(1 - \rho_2)}$ /d	allometric scalar
	$\rho_2$	0.77	...	allometric exponent
	$k_e$	0.61	...	intake coefficient
Mortality	$\mu_0$	0.01	d $^{-1}$	background rate
	$q_s$	0.2	...	starvation condition
	$s$	1	...	starvation coefficient
Resource	$R$		L $^{-1}$	resource population density
	$r$	0.1	d $^{-1}$	population growth rate
	$K$	100.0	L $^{-1}$	carrying capacity
	$m$	$3.0 \times 10^{-5}$	g	wet mass 1.0 per-mm-long <i>Daphnia</i>

Notes: All parameters except  $Y$ ,  $r$ , and  $K$  refer to individual-level processes. For the parameters that are varied between runs of the model, the default value is given in parentheses.

† Source of values = Claessen et al. (2000).

the remainder ( $E_g$ ) is allocated to irreversible mass ( $x$ ) and reversible mass ( $y$ ). The proportion ( $f$ ) of the remainder that is allocated to irreversible mass depends on the individual's condition ( $y/x$ ) (Table 2). The complement is allocated to reversible mass  $y$ . An individual is assumed to allocate a larger proportion to reversible mass if it currently has a lower condition. The allocation rule is designed in such a way that as irreversible mass increases, the ratio  $y/x$  increases asymptotically towards a maximum, which is  $q_j$  for juveniles and  $q_A$  for adults (see Persson et al. 1998).

Whenever the acquired energy does not suffice to cover maintenance requirements (i.e.,  $E_g < 0$ ), an individual converts reversible mass into energy to balance the metabolic rate. Note that starving individuals decrease in body mass while their length remains constant, since length is a function of irreversible mass. Mature individuals are assumed to starve away their gonads before starving somatic reserves. Individuals suffer starvation mortality when their condition decreases below a critical threshold. We assume that the mortality rate due to starvation ( $\mu_s$ ) is positive whenever the condition drops below  $y = q_s x$ , and increases to infinity as  $y$  decreases to zero (Table 2).

The size at maturation is defined in terms of irreversible body mass,  $x_f$ . Mature individuals ( $x \geq x_f$ )

allocate a larger proportion of their energy to reversible mass than do juveniles (that is,  $q_A > q_j$ ). We assume that the maximum amount of somatic reversible mass that an adult can attain is  $y = q_A x$  and that the amount of reversible mass it has on top of this is gonad mass. At the start of a growing season, all mature individuals which have built up gonads (i.e.,  $y > q_j x$ ) reproduce. Fecundity is calculated by dividing the amount of gonad mass (i.e.,  $y - q_j x$ ), multiplied with a conversion efficiency ( $e_r$ ), by the mass of a single newborn.

The mortality rate is assumed to be the sum of the starvation mortality rate ( $\mu_s$ ), a mortality rate due to cannibalism ( $\mu_c$ ), and a background mortality rate ( $\mu_0$ ) (Table 2). The rate at which individuals fall victim to cannibalism ( $\mu_c$ ) depends on the density of potential cannibals and their attack rates, which in turn depend on the lengths of both victim and the cannibals. The cannibalistic interaction will be discussed in more detail in *The predation window*, below.

In spring, the total production of newborns is the sum of the per capita fecundities of all adult individuals. Together, the young-of-the-year (YOY) form a new cohort. They are assumed to be born at the same moment, with identical body mass. An important consequence of pulsed reproduction is that the population consists of discrete cohorts. We assume that individuals

within a cohort experience the same environmental conditions, so that their development is identical. In simulations, cohorts with a density below a trivial threshold (which varied between  $10^{-20}$  and  $10^{-12}$  individuals per liter) were considered extinct. The result of this assumption was that the number of coexisting cohorts generally remained below 50 although the number of cohorts in the population in principle is unbounded. Note that the number of cohorts may vary over time.

The primary, zooplankton resource is modeled as an unstructured population with semi-chemostat dynamics (Table 2). Size-dependent competition for this resource emerges from the scaling of individual vital rates with body size. Smaller individuals have an energy advantage compared to larger ones, because metabolic requirements increase faster with body size than does the foraging capacity. The decrease of the attack rate beyond the optimal size (i.e.,  $L = 94$  mm) enhances the effect, but is not necessary for it. As a consequence, smaller individuals can sustain themselves at a lower resource density than larger ones. Given the dependence of the resource density on consumer density, abundant small individuals may therefore outcompete larger ones by depletion of the zooplankton population. The population-dynamic consequences of size-dependent competition are treated in detail in Persson et al. (1998).

*The predation window.*—Based on empirical data on Eurasian perch and other piscivorous fish species (Christensen 1996, Mittelbach and Persson 1998, Lundvall et al. 1999, Persson et al. 2000) we assume that an individual can take conspecific prey of a given size if the ratio of prey length and predator length is between a lower limit ( $\delta$ ) and an upper limit ( $\varepsilon$ ) (Claessen et al. 2000). We refer to the range of prey lengths a predator can take as the “predation window.” Supported by results from laboratory experiments (Lundvall et al. 1999) we assume that the optimal victim length is a fixed proportion  $\phi$  of the cannibal length, with  $\delta < \phi < \varepsilon$  (Fig. 1).

We assume that the attack rate of a cannibal on victims of a given length depends on the lengths of both cannibal and victim. For the sake of clarity, we introduce the symbols  $c$  and  $v$  as synonyms for the lengths  $L$  of cannibal and victim, respectively (Table 2). We model the cannibalistic attack rate as the product of a maximum and a relative attack rate. The maximum attack rate is the attack rate for victims of the optimal length  $v = \phi c$ . We assume it to be an increasing, allometric function of cannibal length, given by  $\beta c^\sigma$  with  $\sigma = 0.6$  (Fig. 1). The relative attack rate accounts for non-optimal victim sizes. From the optimal victim length  $v = \phi c$  it decreases linearly with victim length  $v$  from 1 to 0 at the boundaries of the cannibalism window. Over the cannibalism window the relative attack rate thus resembles a tent function (Fig. 1).

For a given shape of the predation window (that is,

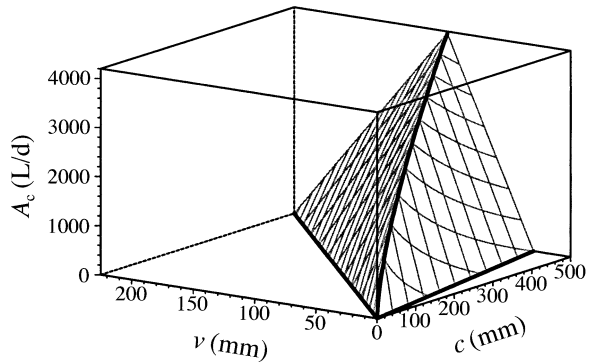


FIG. 1. The cannibalistic attack rate  $A_c$  (Table 2) as a function of cannibal length ( $c$ ) and victim length ( $v$ ), parameterized for Eurasian perch ( $\delta = 0.06$ ,  $\phi = 0.2$ ,  $\varepsilon = 0.45$ ,  $\sigma = 0.6$ ,  $\beta = 100$  [see Table 3 for definition]; cf. Fig. 1 in Claessen et al. [2000]). The two thick lines at the base represent the lower ( $v = \delta c$ ) and upper ( $v = \varepsilon c$ ) limits of the predation window, respectively. For victims of the optimal length ( $v = \phi c$ ), cannibals of length  $c$  have the maximum cannibalistic attack rate ( $A_c = \beta c^\sigma$ ), indicated by the thick curve at the ridge of the surface.

for given values of  $\delta$ ,  $\varepsilon$ , and  $\phi$ ), the parameters  $\beta$  and  $\sigma$  determine the absolute value of the cannibalistic attack-rate function. With  $\beta = 0$  the model reduces to a size-structured consumer–resource model without cannibalism (cf. Persson et al. 1998). A higher value of  $\beta$  corresponds to more voracious cannibalism. The attack rate of a cannibal of a given size on a victim of a given size depends linearly on  $\beta$ . Therefore,  $\beta$  is referred to as the “cannibalistic voracity.”

#### Methods

The model was studied numerically using the “Escalator Boxcar Train” method developed by de Roos et al. (1992) and de Roos (1997). In order to investigate the effect of the predation window, we study the dependence of the asymptotic population dynamics on the parameters  $\beta$ ,  $\delta$ , and  $\varepsilon$ . The patterns of dynamics are summarized in bifurcation diagrams, by delineating regions in parameter space with qualitatively similar population dynamics (e.g., Fig. 2). The patterns in the bifurcation diagrams are interpreted by closely studying time series of population dynamics in different parts of parameter space. This enables us to identify biological mechanisms that are responsible for the different types of population dynamics. Thus we can explain differences between patterns of populations dynamics in terms of processes at the individual level, such as the presence or absence of cannibalistic interactions between abundant cohorts in the population.

#### RESULTS

The impact of cannibalism on population dynamics can be studied by comparing population dynamics excluding cannibalism ( $\beta = 0$ ) with population dynamics that result from various levels of cannibalism ( $\beta > 0$ ).

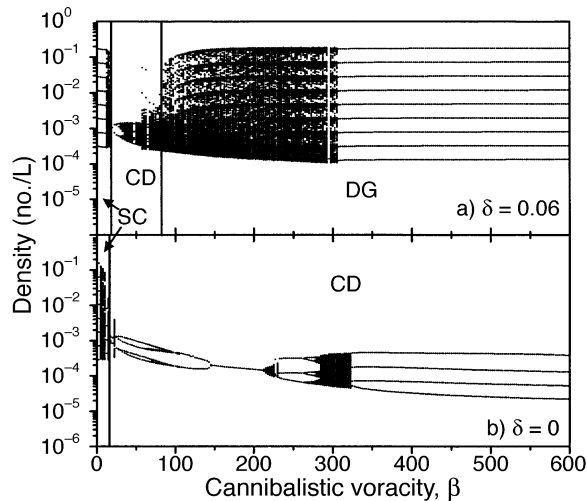


FIG. 2. Bifurcation diagrams for two different values of the lower limit of the predation window,  $\delta$ : (a)  $\delta = 0.06$ ; (b)  $\delta = 0.0$ . In both panels the upper limit of the predation window  $\varepsilon = 0.42$ , the optimum of the predation window  $\phi = 0.15$ , and other parameters are as in Table 3. For any value of  $\beta$  (cannibalistic voracity), the model was run for 800 yr, and the population state was sampled during the last 400 yr. The figure shows the number of individuals in the population, excluding young-of-the-year, at the first day of each year. Abbreviations: SC = single-cohort cycles, CD = cannibal-driven dynamics; DG = dwarfs-and-giants dynamics.

In a recent publication, Claessen et al. (2000) studied the impact of cannibalism on population dynamics for the case of  $\delta$  (the lower limit of the predation window) = 0.06 and  $\varepsilon$  (the upper limit of the predation window) = 0.45, corresponding to the piscivory window of Eurasian perch. Here we first briefly review their results, introducing three types of population dynamics. In the next section we give a more elaborate description of the types of population dynamics and map their occurrence depending on the parameters  $\beta$  and  $\delta$ .

Claessen et al. (2000) found that without cannibalism, as well as with weak cannibalism, 8-yr large-amplitude cycles prevail with only one cohort present in the population, referred to as single-cohort (SC) cycles (Fig. 2a). These cycles are analogous to generation cycles (Gurney and Nisbet 1985), and result from the competitive superiority of small individuals. With intermediately voracious cannibalism, larger individuals reduce intercohort competition by killing small individuals. Cannibalism may thus reduce size-dependent competition, resulting in coexistence of juveniles and 100–200 mm long adults. We refer to this type of population dynamics as “cannibal-driven (CD) dynamics” (Fig. 2a). For high values of the cannibalistic voracity ( $\beta$ ), Claessen et al. (2000) found large-amplitude 9-yr cycles (Fig. 2a). In these cycles the population has a bimodal size distribution. Individuals in the so-called “giant” size class grow fast and reach giant sizes (>300 mm) on a cannibalistic diet. Individuals in the “dwarf” size class grow slowly and remain relatively

small. Such cycles are referred to as “dwarfs-and-giants (DG) cycles” (Claessen et al. 2000). For lower  $\beta$  irregular dynamics are found (Fig. 2a) where periods of cannibal-driven dynamics, without giants, alternate with periods resembling DG cycles, with giants. We refer to this irregular dynamics as well as the 9-yr cycles as “dwarfs-and-giants (DG) dynamics.”

#### Effects of the minimum prey size ratio ( $\delta$ )

The effects of the minimum prey size ratio will be studied by varying  $\delta$  and  $\beta$  while holding the other parameters of the predation window constant at  $\varepsilon = 0.42$  and  $\phi$  (the optimum of the predation window) = 0.15. These values deviate slightly from the default set for Eurasian perch ( $\varepsilon = 0.45$  and  $\phi = 0.2$ ), but they produce qualitatively the same results. The patterns are more transparent with the chosen values because the effect of changing the lower limit  $\delta$  becomes more outspoken when the optimum ratio  $\phi$  is closer to the lower limit.

We first illustrate the effect of  $\delta$  by comparing two different  $\delta$  values (Fig. 2). A striking effect of lowering  $\delta$  from 0.06 to 0 is that all DG dynamics are replaced by CD dynamics. The amplitude of fluctuations is much smaller with  $\delta = 0$  than with  $\delta = 0.06$ . This is a first indication that the stabilizing influence of cannibalism is stronger with smaller values of  $\delta$ . Fig. 3 summarizes a large number of bifurcation diagrams as presented in

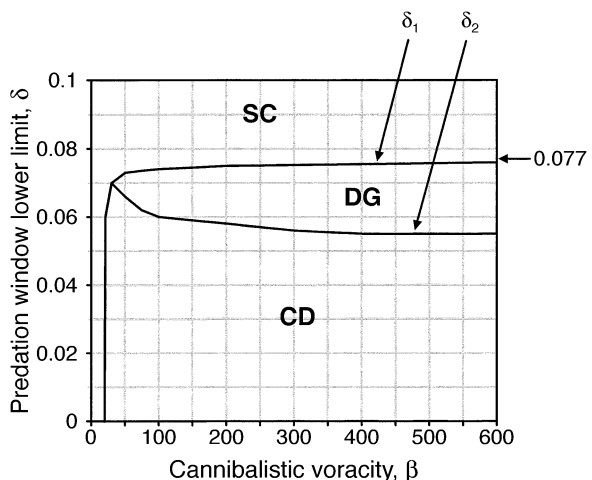


FIG. 3. Regions with qualitatively similar population dynamics in the  $\beta$ - $\delta$  plane. Here the optimum of the predation window  $\phi = 0.15$ , the upper limit of the predation window  $\varepsilon = 0.42$ , and other parameters are as in Table 3. Abbreviations: SC = single-cohort cycles; DG = dwarfs-and-giants dynamics; CD = cannibal-driven dynamics. At smaller  $\beta$  (cannibalistic voracity) values ( $\beta \leq 300$ ), the DG region includes dynamics where dwarfs-and-giants cycles alternated with periods of cannibal-driven dynamics. For explanation of the boundaries  $\delta_1$  and  $\delta_2$ , see *Results: Effects of the minimum prey size ratio: Boundaries between regions*. Grid lines indicate parameter values of the bifurcation transects used. In horizontal transects,  $\beta$  is varied with steps of 5. In vertical transects,  $\delta$  is varied with steps of 0.002.

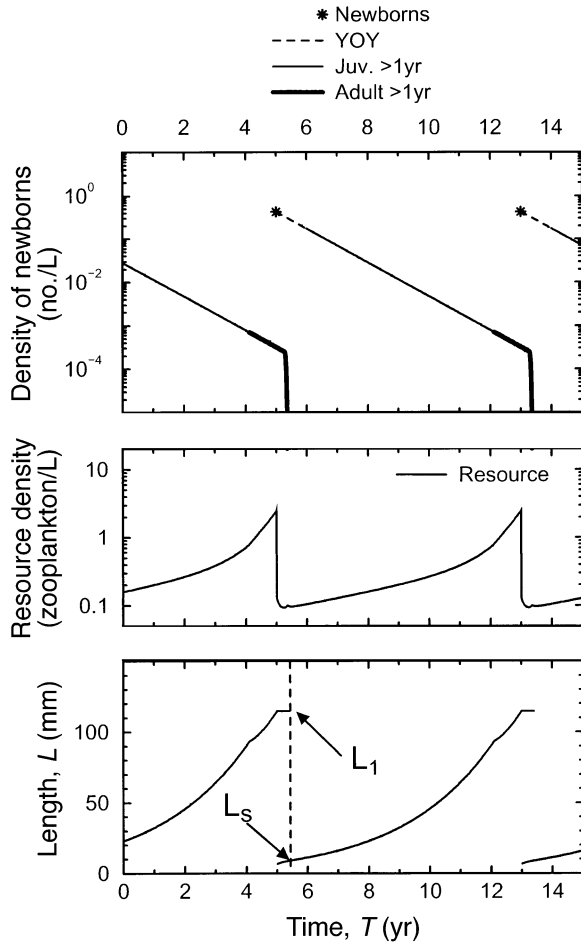


FIG. 4. Single-cohort (SC) cycles for  $\beta = 0$ : (top panel) total population density of newborns, young-of-the-year (YOY), juveniles >1-yr old and adults; (middle panel) resource (zooplankton) density. Note the logarithmic scale on the y-axes of these two panels. (Lower panel) Growth trajectories of all present cohorts. The vertical dashed line marks the time of extinction of the adult cohort (year  $T = 5$ , day  $\tau_s = 115$  mm). The arrows point out the length of the adults ( $L_1 = 115$  mm) and of the recruits ( $L_s = 8.85$  mm) at that time.

Fig. 2, with  $\beta$  and  $\delta$  as bifurcation parameters. We have subdivided the  $\beta$ - $\delta$  plane into three regions, delineating the three types of population dynamics mentioned above. In the next section we explain the patterns of population dynamics in each region in Figs. 2 and 3. Understanding the mechanisms that cause the different patterns helps to understand the boundaries between the different regions.

*Types of population dynamics.*—For very weak cannibalism (low  $\beta$ ) or a high lower limit of the predation window ( $\delta > \delta_1$ ), our model predicts single-cohort cycles (Figs. 2 and 3). An extensive study of such dynamics can be found in Persson et al. (1998) and de Roos and Persson (2001). An example is given in Fig. 4. This type of population dynamics results from the competitive superiority of small individuals to larger

ones. Because of their lower metabolic rate newborns can sustain themselves on a lower zooplankton density than adults, despite the newborns' lower attack rate (Persson et al. 1998, Hjelm and Persson 2001). Each new generation outcompetes the previous one by depleting the resource density below the level that adults require for their maintenance. In these cycles individual growth is slow (Fig. 4) due to high intracohort competition. Individuals reach maturity in their seventh year, which explains the cycle period of eight years. The mechanism of SC cycles does not depend on the dome shape of the planktivory attack-rate function, but the cycle period depends on the optimum size  $x_{opt}$  (Persson et al. 1998). Critical to the SC cycles is that cannibalism by adults does not cause a high mortality rate on YOY (young-of-the-year). SC cycles are hence found for low  $\beta$  or high  $\delta$ . Below, the prolonged resource depletion caused by a dense, juvenile cohort is referred to as a "long-term resource depletion."

For intermediate values of  $\beta$ , and a sufficiently small  $\delta$  (Figs. 2 and 3), the model predicts cannibal-driven dynamics. Within the CD region we found regular cycles with periods between one and six years, as well as irregular dynamics (Fig. 2). Although details may differ, dynamics in this region are always governed by the cannibalistic interaction, in the sense that high cannibalistic mortality of YOY prevents YOY from outcompeting the adults through long-term resource depletions. In Fig. 5 the high YOY mortality is reflected by the steep decline of YOY density, compared to the constant background mortality of the adult size class. The cannibals of the YOY are large juveniles and small adults ( $L \sim 80$ – $200$  mm). The population has a relatively stable size distribution and the density of the adult size class fluctuates with a small amplitude compared to SC dynamics. The CD dynamics are characterized by coexistence of many cohorts and fast individual growth during the first two or three years, followed by several years of slower growth (Fig. 5).

We illustrate some details of CD dynamics with an example of a 4-yr cycle (Fig. 5), which is found in a large part of the CD region ( $\beta > 320$  in Fig. 2b). Every four years a cohort is born that, despite its low initial density, dominates the population numerically during the next four years (e.g., Fig. 5,  $T = 1$ ). The reason for its abundance is that it suffers relatively low cannibalistic mortality as YOY (Fig. 5). It controls the resource level except during the short depletions caused by reproductive pulses. During its first year, the dominant cohort serves as an ample food source for the largest individuals in the population. This causes the cannibals to grow beyond the maximum sustainable size on zooplankton, and the cannibals starve to death when the victims have left their predation window (Fig. 5,  $T \sim 2$ – $3$ ). Cannibalism by the dominant cohort decimates the next three year classes of which very few individuals survive to maturity (Fig. 5). The density of the dominant cohort decreases by background mortality



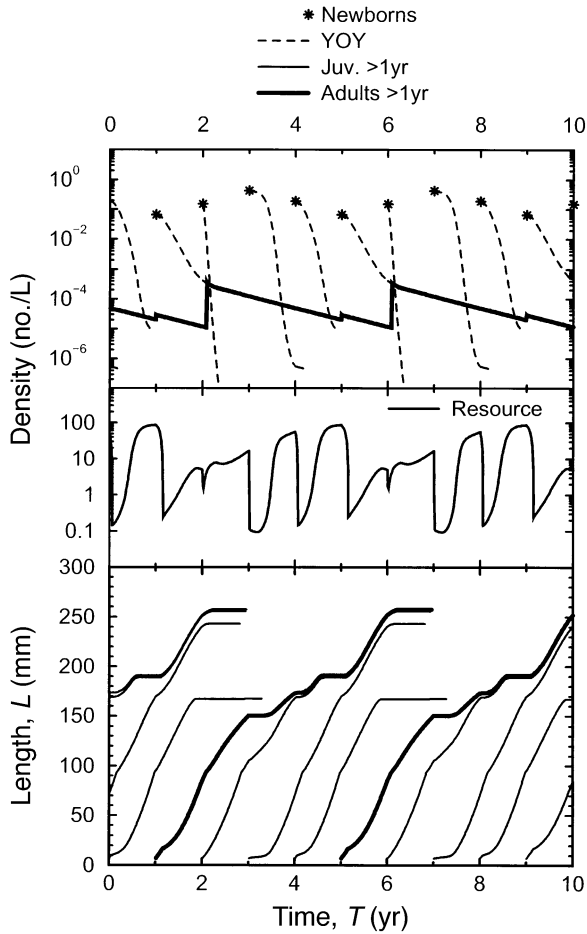


FIG. 5. Example of a stable 4-yr cycle in the cannibal-driven (CD) region ( $\beta = 700$ ,  $\delta = 0.054$ ,  $\varepsilon = 0.42$ ,  $\phi = 0.15$ ). Format and symbols are as in Fig. 4. Growth trajectories of two successive dominant cohorts (born at  $T = 1$ ,  $T = 5$ ) are drawn thicker.

and when the fourth pulse is born ( $T = 5$ ) the impact on YOY survival is relatively small. As a consequence, this YOY cohort will be the next dominant cohort. Although this cohort is numerically dominant, it is not abundant enough to outcompete the older year classes, which is typical for CD dynamics.

If the lower limit of the predation window is between two critical values ( $\delta_1 > \delta > \delta_2$ ), dwarfs-and-giants dynamics are found for most  $\beta$  values (Fig. 2b, Fig. 3). In the  $\beta$ - $\delta$  plane the DG region forms the transition zone between the SC region and the CD region (Fig. 3). Features of both SC and CD dynamics, i.e., severe intercohort competition on the one hand and YOY regulation by cannibalism on the other, are important aspects of DG dynamics. DG dynamics are characterized by emergence of dynamically induced giants feeding on a slowly growing, planktivorous size class, referred to as “dwarfs” (Claessen et al. 2000). DG dynamics can be either regular or irregular (Fig. 2a). In a regular dwarfs-and-giants cycle, an abundant, slowly growing

cohort of dwarfs produces two pulses of offspring in two subsequent years (Fig. 6, e.g.,  $T = 2, 3$ ). Each pulse of newborns results in a sudden depletion of the resource. The dwarf cohort survives competition with their first pulse of offspring because they cannibalize most of it. Consequently the resource density recovers, enabling the adult dwarfs to grow to a larger size before they reproduce again (Fig. 6, lower panel). The second time ( $T = 3$ ) the resource depletion causes their starvation death before the YOY enter their predation window. The few survivors of the first pulse of offspring (now 1 yr old) survive the long-term resource depletion caused by the second pulse because their size allows them to cannibalize the newborns. Cannibalism on the

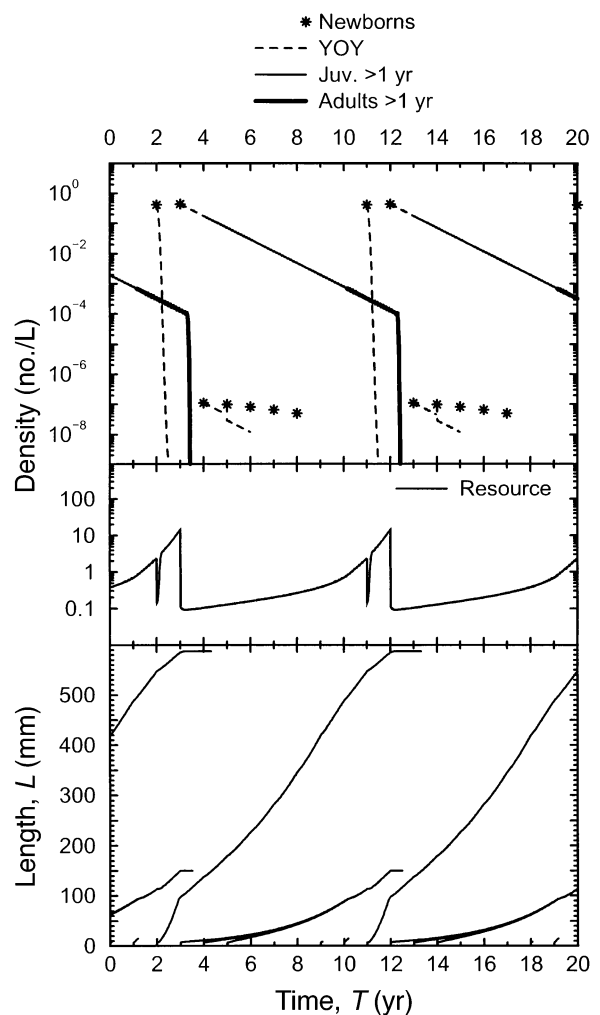


FIG. 6. Example of a stable dwarfs-and-giants (DG) cycle ( $\beta = 400$ ,  $\delta = 0.056$ ,  $\phi = 0.15$ ). Format and symbols are as in Fig. 4. At first reproduction (e.g.,  $T = 2$ ), the length of dwarfs ( $L_1 = 114$ ) is small enough to decimate the young-of-the-year (YOY) cohort. At second reproduction (e.g.,  $T = 3$ ), the length of the dwarfs is too large ( $L_2 = 150$ ) to cannibalize the YOY. The dwarf cohort goes extinct (at day  $\tau_S = 42$ ), whereas the survivors of the first offspring pulse utilize the new dwarf cohort to become giants.

new dwarf cohort enables these individuals to reach giant sizes (Fig. 6, lower panel). Close to the boundary of the CD region (Fig. 2a,  $\beta \approx 300$ ) dwarfs-and-giants cycles are irregularly alternated by periods with dynamics resembling CD dynamics. The dynamics are not shown here, but see Fig. 8 in Claessen et al. (2000) for an example and extensive discussion. The CD-like periods are ended when an abundant YOY cohort depletes the resource density for a prolonged period, out-competing the cannibal size class, which maintained the population in the stabilized state. A few individuals from the cannibal size class survive and become giants by feeding on the abundant dwarf cohort.

*Boundaries between regions.*—The boundary between the SC region and the DG region (Fig. 3; curve  $\delta_1$ ) can be understood by considering the interaction between newborns and their parents in stable SC cycles (Fig. 4). Immediately after reproduction, the offspring cohort depletes the resource, which forces the mature individuals to starve away their reserves; their reversible mass  $y$  decreases whereas the irreversible mass  $x$  remains constant. Because length is assumed to be a function of  $x$  only, the length of adults remains constant, referred to as  $L_1$  (Fig. 4). After  $\tau_s$  days the reversible mass of adults reaches the starvation threshold  $y = q_s x$ , and the adult cohort goes extinct due to starvation mortality. The length of the young-of-the-year at that moment will be referred to as  $L_s$  (Fig. 4).

Now consider the prospects for cannibalism in the context of these SC cycles. If the length at birth  $L_b$  is outside the adults' predation window (that is, if  $L_b < \delta L_1$ , see Table 2), then newborns are temporarily invulnerable to cannibalism. As long as the YOY are invulnerable (i.e., their length  $< \delta L_1$ ) their abundance ensures that the adults continue to starve at the constant length of  $L_1$ . The YOY will not be cannibalized at all if the adults die of starvation before the YOY reach the length  $\delta L_1$ . In other words, adults never encounter the YOY if

$$\delta > \frac{L_s}{L_1}. \tag{1}$$

If, on the other hand, the lower limit of the predation window is smaller than  $L_s/L_1$ , newborns are cannibalized by adults and the mechanism of the SC cycles is weakened. Thus, for sufficiently high  $\beta$  we expect no SC cycles below this critical value of  $\delta$ . Fig. 4 illustrates that with the perch parameters  $L_s/L_1 = 0.077$ , and bifurcation runs show that the boundary between the SC region and DG region approaches this value asymptotically as  $\beta$  is increased (Fig. 3: curve  $\delta_1$ ).

Simulation studies show that the values of  $L_1$ ,  $\tau_s$ , and  $L_s$  are independent of the resource parameters  $r$  and  $K$  except for very small values of  $r$  and  $K$  (i.e., close to the persistence boundary of the cannibal population). This means that the boundary between SC and DG population dynamics relates to characteristics of the

cannibal species alone, and not to the specifics of the zooplankton dynamics.

The boundary between the DG dynamics and the CD dynamics (Fig. 3: curve  $\delta_2$ ) can be understood in a similar way. As described above, in stable dwarfs-and-giants cycles the dwarf cohort produces two pulses of offspring in two subsequent years (Fig. 6). The lengths of the adult dwarfs at these two reproduction events will be referred to as  $L_1$  and  $L_2$ , respectively. We have already seen that since  $\delta < L_s/L_1$  the first newborns are decimated by the dwarfs. Because the resource density is high in between the two reproduction events, the adult dwarfs grow, and hence  $L_2 > L_1$ . In a stable DG cycle, the dwarfs starve to death before the second cohort of newborns enters their predation window. In analogy with the above reasoning for  $\delta_1$ , our conjecture is that the critical value  $\delta_2$  is that value below which newborns enter the predation window of dwarfs of length  $L_2$  before the latter starve to death. From Fig. 6 we can obtain the values  $\tau_s = 42$  d,  $L_2 = 150$  mm, and  $L_s = 9$  mm. The expected value of  $\delta_2$  is hence  $L_s/L_2 = 0.06$ .

Fig. 3 shows that the asymptotic value of  $\delta_2$  is lower. There are three reasons why our estimate of  $\delta_2$  is not very accurate. First, the length  $L_2$  and the corresponding values of  $\tau_s$  and  $L_s$  are not independent of the parameters  $\beta$  and  $\delta$  because  $L_2$  depends on cannibalism on the YOY. Second, the dynamics on either side of the boundary  $\delta_2$  are most often not regular so that we cannot obtain general estimates of  $L_2$ ,  $\tau_s$  and  $L_s$ . Third, due to the large metabolic demands of an individual of length  $L_2 = 150$  mm (which corresponds to an irreversible mass of  $x = 20.8$  g) such an individual needs much more energy to recover from starvation than an individual of length  $L_1 = 114$  mm ( $x = 8.8$  g). The boundary should hence not be expected at  $\delta = L_s/L_2$  but at a somewhat smaller value.

*Effects of the maximum prey size ratio ( $\epsilon$ )*

We first study the effect of the upper limit of the predation window ( $\epsilon$ ) assuming  $\delta = 0$ ,  $\phi = 0.2$ , and a fixed cannibalistic voracity  $\beta = 200$ . With the default value of  $\epsilon$ , these parameters are in the CD region and result in stable fixed-point dynamics (cf. Fig. 2b,  $\beta = 150 \dots 210$ ). Generally, if the lower limit of the predation window ( $\delta$ ) is chosen in such a way that cannibal-driven population dynamics result, the effect of the upper limit on overall population densities is relatively small. For example, Fig. 7a shows that in a large range of  $\epsilon$  fixed-point dynamics are found. Also outside this range the population density remains below  $10^{-2}$ , characteristic of CD dynamics (cf. Fig. 2).

Contrary to the small effect on overall population densities, the effect of  $\epsilon$  on population size distribution and individual life history is rather drastic. The dependence of the length of the oldest individuals in the population on  $\epsilon$  reflects this result (Fig. 7b). Near a critical value of  $\epsilon^* \sim 0.65$  the ultimate of size of in-

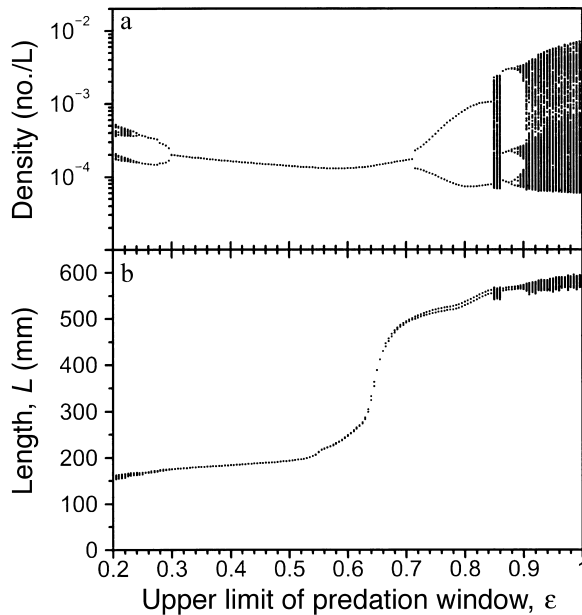


FIG. 7. Bifurcation diagram of parameter  $\varepsilon$  (the upper limit of the predation window), with  $\beta = 200$ ,  $\delta = 0$ ,  $\phi = 0.2$  and other parameters as in Table 3. For any value of  $\varepsilon$ , the model was run for 800 yr, and the population state was sampled during the last 400 yr. (a) Population density at the first day of each year, excluding young-of-the-year. (b) Length of the longest individual at the first day of each year. For all values of  $\varepsilon$  in the range 0.2–1, cannibal-driven (CD) dynamics are found (fixed point in the range  $0.3 < \varepsilon < 0.71$ ). Around the critical value  $\varepsilon^* = 0.65$  the asymptotic length in the population increases drastically.

dividuals suddenly increases to a size that is similar to the ultimate size of giants in DG dynamics (Fig. 6). Note that the change in individual length occurs in a range of  $\varepsilon$  values without significant change of overall population densities (Fig. 7a). Individuals with  $L > 200$  depend fully on piscivory, since their planktivorous attack rate is negligible. Apparently, in the region with  $\varepsilon > \varepsilon^*$  individuals can reach giant sizes without the dynamic induction such as in DG dynamics.

We investigate the mechanism for the sudden change in population structure by considering population size distributions for five different  $\varepsilon$  values within the range of stable fixed-point dynamics (Fig. 8). Fig. 8a shows the population structure at the first day of each year for  $\varepsilon = 0.4$ . From the figure it can be inferred that individuals grow fast during the first two years and then gradually reach an ultimate size of  $L_\infty = 186$  mm. The decreasing per capita fecundity of the larger cohorts indicates that these individuals have a low condition. Fig. 9a shows that planktivory provides the major contribution to the individual growth rate, and that the effect of the energy gain from cannibalism (of YOY victims only) on ultimate individual size is small. The population structure for  $\varepsilon = 0.5$  (Fig. 8b), is very similar to the case of  $\varepsilon = 0.4$ , except that the ultimate size is slightly higher, which can be attributed to an in-

creased contribution of the cannibalistic energy gain (Fig. 9b). Fig. 9b also indicates that, if there were any individuals with a length between 400–530 mm, they had a positive net growth rate, solely due to the energy gain from cannibalism. We refer to this length interval with positive average net growth due to cannibalism as the “piscivory niche.” The length interval for which planktivory has a significant contribution is referred to as the “planktivory niche” (i.e.,  $L < 200$ , Fig. 9). With  $\varepsilon = 0.5$  the planktivory and piscivory niches are separated from each other by a size interval with negative growth rates, which makes the piscivory niche unreachable. With  $\varepsilon = 0.4$ , the piscivory niche does not exist at all (Fig. 9a).

For  $\varepsilon = 0.6$  most individuals still do not grow beyond 200 mm (Fig. 8c). Yet the actual ultimate individual size is drastically larger ( $>400$  mm, Fig. 8c). The pop-

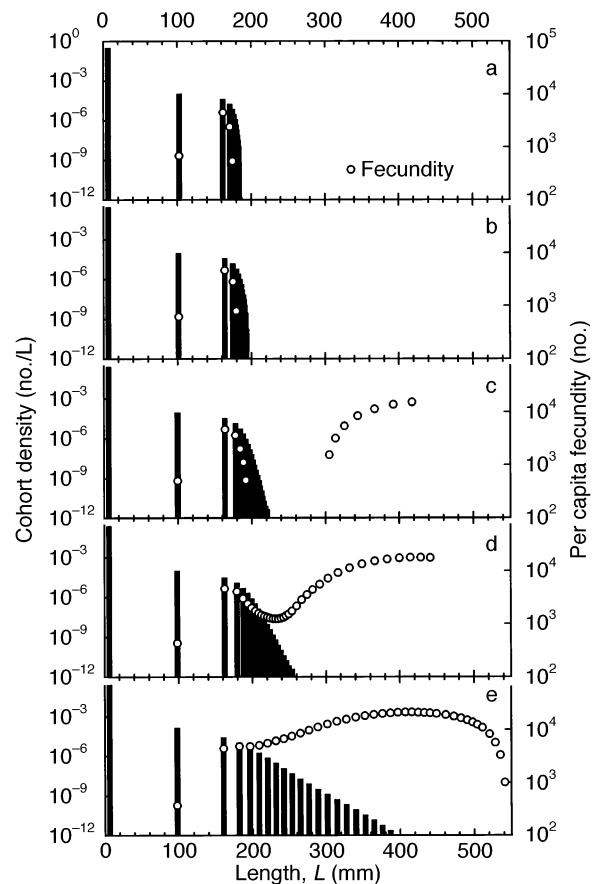


FIG. 8. The population states at the first day of each year, for different values of the upper limit of the predation window,  $\varepsilon$ : (a)  $\varepsilon = 0.4$ , (b)  $\varepsilon = 0.5$ , (c)  $\varepsilon = 0.6$ , (d)  $\varepsilon = 0.64$ , (e)  $\varepsilon = 0.7$ . Other parameters:  $\beta = 200$ ,  $\delta = 0$ ,  $\phi = 0.2$ , and as in Table 3. For these parameter values, the population dynamics converge quickly to a fixed point (Fig. 7). The histograms indicate densities of size classes. The open circles indicate the per capita fecundity of individuals in each cohort (age class). Although the densities of size classes  $< 10^{-12} L^{-1}$  are not shown, their fecundity is plotted as an indication of the presence of individuals, and their condition.

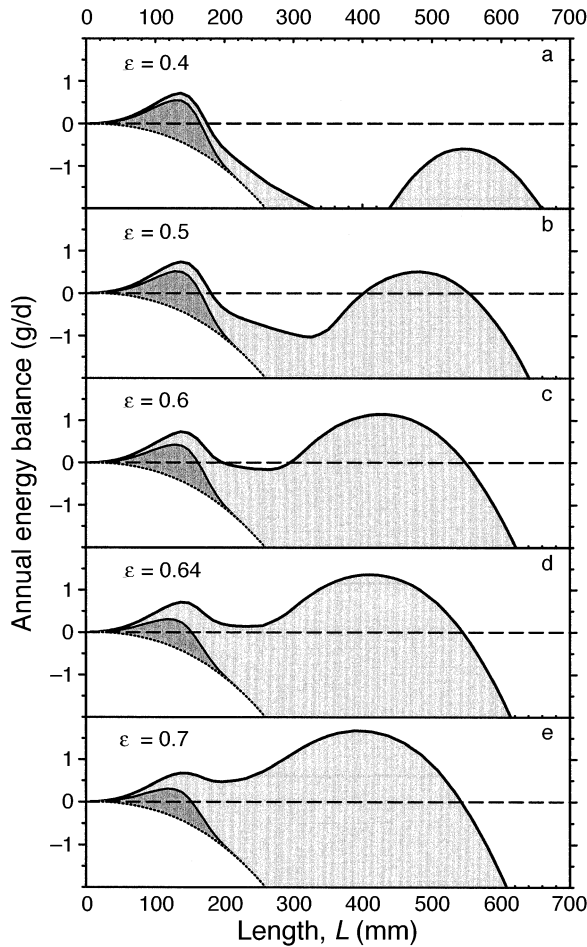


FIG. 9. The size-dependent annual energy balance for different values of  $\epsilon$ , the upper limit of the predation window. Other parameters are as in Figs. 7 and 8. The net growth rate (thick solid line) is obtained by adding the intake rate (all dark and light gray areas) to the (negative) metabolic rate (dotted line). The distance between the dotted and thick solid line corresponds to the total energy intake rate. The contributions to intake from planktivory (dark gray) and piscivory (light gray) are indicated. All rates are averaged over the entire growing season and expressed as growth per day. For the calculations we assumed standard condition ( $y = q_p x$ ). The size range with a significant contribution from planktivory is referred to as the "planktivory niche" (i.e.,  $L < 200$  mm). The size range with positive energy balance beyond the planktivory niche is referred to as the "piscivory niche."

ulation contains a very few very long individuals, whose density is too low to appear in Fig. 8c. Their existence is apparent from the graph of fecundity vs. length. It appears that starvation enables individuals to grow through the bottleneck between the planktivory and piscivory niches. While for individuals with the maximum amount of somatic reserves ( $y = q_p x$ ), the net average growth rate in the gap between the two niches is negative (Fig. 9c), for individuals at the starvation threshold ( $y = q_s x$ ) it is positive (not shown). Note that in our model we assume that metabolic costs

depend on the sum of irreversible and reversible mass (Table 2). Fig. 8c shows that the individuals in the gap cannot reproduce, which implies that they have a low condition ( $y < q_p x$ ). Thus, by starving away reserves (and gonads), and thereby reducing metabolic costs, individuals can reach the piscivory niche, although it takes them so long that only a very few survive until that time. Once in the piscivory niche ( $L > 300$  mm, Fig. 9c) their condition increases, and they start reproducing again (Fig. 8c). For even larger values of  $\epsilon$ , the interval with negative net growth at  $y = q_p x$  disappears (Fig. 9d) and individuals reach the piscivory niche without completely losing fecundity (Fig. 8d). Close to the critical  $\epsilon$  value (e.g.,  $\epsilon = 0.64$ ) the bottleneck is still noticeable by the reduced fecundity and a decreased growth rate. Here, the number of individuals reaching the piscivory niche is still very small (Fig. 8d). For large values of  $\epsilon$  the effect of the bottleneck is negligible; the population size distribution is very wide and relatively many individuals reach the piscivory niche (Fig. 8e).

As mentioned before, despite the impact of  $\epsilon$  on population structure and individual life history, the effect on overall population densities is minor. The main reason for this is that the population dynamics in the CD region are almost completely determined by the interaction between YOY, 1-yr-old and 2-yr-old individuals. A large value of  $\epsilon$  mainly affects individuals of  $L > 180$  mm, which are often at least three years old (e.g., Fig. 8e).

The generality of the effect of  $\epsilon$  is investigated by comparing a large number of bifurcation diagrams with  $\epsilon$  and  $\beta$  as bifurcation parameters, summarized in Fig. 10. Cannibal-driven population dynamics are found for most values of  $\beta$  and  $\epsilon$ . Only for very small  $\beta$  do we find SC cycles. Bifurcation diagrams such as Fig. 2b are qualitatively the same for different values of  $\epsilon$ . Only the locations ( $\beta$  values) of the bifurcations depend on  $\epsilon$ . From this we conclude that  $\epsilon$  has little impact on overall population dynamics. The critical value of  $\epsilon$  where the population size distribution changes abruptly (e.g., Fig. 7:  $\epsilon \sim 0.65$ ) is marked as the curve  $\epsilon^*$  in Fig. 10. The curve separates a parameter region ( $\epsilon > \epsilon^*$ ) where the piscivory niche is permanently reachable (cf. Fig. 8e) from a region ( $\epsilon < \epsilon^*$ ) where the piscivory niche is unreachable.

Two important conclusions about the piscivory niche can be drawn from Fig. 10. First, the negative slope of the curve  $\epsilon^*$  shows that more voracious piscivores can enter the piscivory niche with a smaller upper limit of the predation window. Second, the existence of the curve  $\epsilon^*$  for all values of  $\beta > 50$  implies that the abrupt opening of the piscivory niche at a critical value  $\epsilon^*$  occurs independently of the periodicity or regularity of the CD dynamics. Figs. 8 and 9 hence represent the simplest case of a more general phenomenon, which does not require fixed-point dynamics. Even with non-fixed-point dynamics Fig. 9 proves to be a useful met-

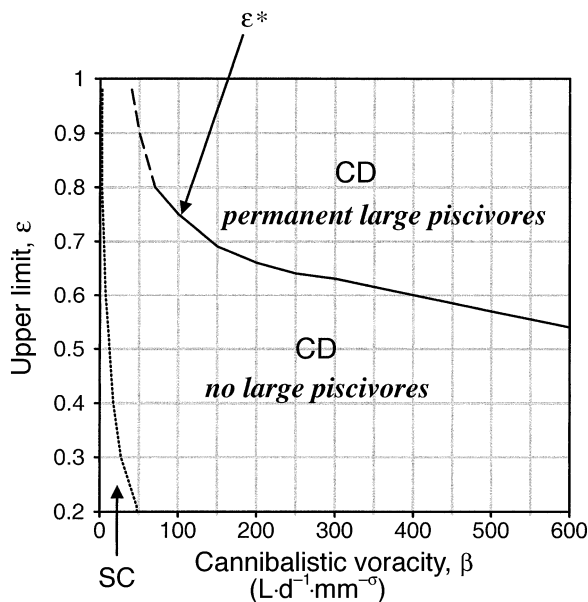


FIG. 10. The occurrence of large piscivores in population dynamics, depending on the parameters  $\beta$  (cannibalistic voracity) and  $\varepsilon$  (upper limit of the predation window). Other parameters are  $\delta = 0$ ,  $\phi = 0.2$ , and as in Table 3. In the region above the curve indicated with  $\varepsilon^*$  piscivores are present permanently in cannibal-driven (CD) dynamics. In the region below  $\varepsilon^*$  they are absent. The curve  $\varepsilon^*$  is dashed for small  $\beta$  because in that region the effect of cannibalism on the asymptotic length is hard to distinguish. Grid lines indicate parameter values of the bifurcation transects used. In horizontal transects  $\beta$  is varied with steps of 5; in vertical transects  $\varepsilon$  is varied with steps of 0.02. SC = single-cohort cycles.

aphor in understanding the system because it explains (1) the abruptness of the change in asymptotic length, and (2) the possible existence of an unreachable piscivory niche for  $\varepsilon$  values close to the critical value  $\varepsilon^*$ .

In fact, the unreachable piscivory niche is the reason why the asymptotic length changes so abruptly at  $\varepsilon^*$ . At this value of  $\varepsilon$  the maximum size in the planktivory niche “merges” with the minimum size in the piscivory niche (cf. Fig. 9), resulting in a single growth trajectory towards the maximum size in the piscivory niche for  $\varepsilon > \varepsilon^*$ . In analogy with bifurcation theory, the merging of the two extreme sizes at  $\varepsilon^*$  corresponds to a saddle-node bifurcation. For values of  $\varepsilon$  in the range with the unreachable piscivory niche (e.g.,  $0.45 \leq \varepsilon \leq 0.62$  in Fig. 9) there is “bistability” of growth trajectories, in the sense that the asymptotic length depends on the initial conditions. However, since all life-history trajectories start with the same initial conditions (i.e., size at birth), all growth trajectories converge to the first asymptotic length, which corresponds to the maximum size in the planktivory niche.

#### DISCUSSION

We studied the impact of the lower ( $\delta$ ) and upper ( $\varepsilon$ ) limits of the predation window on size-structured pop-

ulation dynamics. Although these parameters represent closely related individual-level aspects of predators and prey, we found that the system reacts very differently to changes in  $\delta$  or  $\varepsilon$ . Whereas the lower limit has a strong impact on population dynamics, by determining the stabilizing potential of intraspecific predation, the upper limit primarily affects the individual level, by determining important life-history characteristics. The difference in population-dynamic impact of  $\delta$  and  $\varepsilon$  relates to the importance of young-of-the-year (YOY) for population dynamics. Since the size of newborns is close to the minimum prey size for the bulk of the cannibal size class ( $L = 80\text{--}180$  mm), a small change in  $\delta$  can have major impact on the YOY survival rate. Changing  $\varepsilon$  has no direct impact on YOY survival, and hence little impact on population dynamics. The much larger impact of  $\varepsilon$  on population structure is explained by the importance of the ontogenetic niche shift from planktivory to piscivory for individual life history. Whereas  $\varepsilon$  determines the size at which individuals can switch to piscivory,  $\delta$  only has a minor effect on the ultimate size within the piscivory niche.

We argue that the different reactions of the system to changes in  $\delta$  and  $\varepsilon$  reflect two different aspects of cannibalism, which we refer to as “the two faces of cannibalism.” The negative face of cannibalism is the additional mortality inflicted upon victims. The positive face is the energy gain obtained by cannibals. Our results suggest that there is a mutually exclusive relation between these two aspects. On the one hand, if victim mortality is an important effect of cannibalism, then the cannibals do not gain much energy from it. This type of cannibalism may best be referred to as “infanticide.” On the other hand, the energy gain from cannibalism can only be substantial if cannibalism does not have a major impact on victim mortality. In these terms, a small  $\delta$  promotes the negative face of cannibalism whereas a large  $\varepsilon$  promotes the positive face. Note that within one population the two faces of cannibalism can be important simultaneously, yet not for the same *individuals*. The ontogenetic niche shift from planktivory to piscivory corresponds to a switch between the two “faces” of cannibalism. For example, in Fig. 9e cannibalism by 100-mm-long individuals is mainly infanticide, regulating YOY survival, whereas cannibalism by individuals  $>200$  mm only affects their own growth rate.

For many freshwater fish, macroinvertebrates are an important second resource, accessible mainly for larger individuals (Werner and Gilliam 1984). With a shared second resource, competition still leads to single-cohort (SC) cycles (de Roos and Persson 2001). Also with a second resource exclusive to larger individuals SC dynamics still predominate (M. Vlaar and D. Claessen, *unpublished data*). We expect that size-dependent cannibalism stabilizes SC dynamics with two resources under the same conditions as with a single resource. Therefore we anticipate that the results regarding  $\delta$  still

hold with a second resource. There are indications that macroinvertebrates are important for growth and survival of perch >150 mm (Persson et al. 2000). This may have implications for the effects of  $\varepsilon$ , which we plan to address in future research.

Below, we compare our model predictions with field data. The first section focusses on  $\delta$ , the second on  $\varepsilon$ .

*Model and data: cannibalism vs. intercohort competition*

Comparing empirical data on the lower limit of the predation window for specific species with Fig. 3 and Eq. (1), one can predict whether population dynamics are likely to be stabilized by cannibalism. Whereas values of  $L_1$  (the length at first reproduction) and  $\tau_S$  (the number of days an individual of length  $L_1$  can survive without food) may be relatively easily obtained from field or laboratory data for different species,  $L_S$  (the length of newborns at age  $\tau_S$ ) is hard to estimate due to its dependence on population dynamics and the interaction with the resource density. With a size-structured model of the competitive interaction, parameterized for the species of interest,  $L_S$  can be predicted. With our model for perch we found that the observed lower limit ( $\delta = 0.06$ , Claessen et al. 2000) is in between the two critical values  $\delta_1$  and  $\delta_2$ . Alternatively, using size at birth (or size at first feeding, if more appropriate) as an approximation of  $L_S$  we can formulate a crude rule of thumb. Intraspecific predation may regulate population dynamics only if the lower limit of the predation window ( $\delta$ ) is smaller than the ratio of length at birth and length at maturation, or is at least close to it. As an example, for Arctic char (*Salvelinus alpinus*) length at reproduction is 100–149 mm (Hammar 2000) and length at first feeding  $\sim 20$  mm (Jens Andersson, *personal communication*). The critical value for the lower limit is hence 20/100. The actual lower limit of the predation window is  $\sim 0.15$  (Amundsen 1994), which is well below the critical value. On the basis of  $\delta$ ,  $L_b$ , and  $L_1$  alone, cannibal-driven dynamics can be expected. However, a thorough analysis using a char-specific parameterization of the bioenergetics in the model is necessary before more firm predictions can be made.

In the context of our model predictions it is interesting to compare the single-species population dynamics of two closely related piscivorous fish, yellow perch (*Perca flavescens*) and Eurasian perch (*P. fluviatilis*). The dynamics of the yellow perch population in Crystal Lake (Wisconsin, USA) are characterized by cohort dominance (Sanderson et al. 1999). Repeatedly, a single abundant cohort dominates the population size distribution for several years. Recruitment is virtually absent as long as this cohort is juvenile. After maturation of the dominant cohort, high densities of YOY depress the resource density. The die-off of adults is attributed to intercohort competition with YOY (Sanderson et al. 1999). Despite the presence of cannibalism

in this population, the most important interaction between YOY and adults seems to be competition, favoring YOY (Sanderson et al. 1999). The observed population dynamics resemble single cohort (SC) cycles. In contrast, a detailed empirical study of the dynamics of a Eurasian perch population shows a prominent role for cannibalism and no cohort dominance (Persson et al. 2000). For several years, adults are constantly present and reproduce each year. Despite the evidence for the competitive superiority of YOY, cannibalism reduces YOY densities sufficiently for the adults to survive. However, after a major die-off in the adult size class, successful survival of YOY is observed. This change from an adult-dominated state to a juvenile-dominated state is associated with the emergence of giant cannibals (Claessen et al. 2000, Persson et al. 2000). This pattern of population dynamics resembles the alternation of cannibal-driven dynamics and dwarfs-and-giants (DG) cycles, which our model predicts for parameter values in the DG region.

Our results on the effect of  $\delta$  on population dynamics offer an explanation for these differences in population dynamics. In their interspecific comparison of piscivorous fish, Mittelbach and Persson (1998) show that yellow perch have a smaller gape width than Eurasian perch of the same size. Yellow perch need more time to manipulate prey than Eurasian perch, especially for small relative prey sizes. Data on prey sizes in the diet show that yellow perch has a narrower predation window, with both a higher lower limit ( $\delta$ ) and a smaller upper limit ( $\varepsilon$ ) (Mittelbach and Persson [1998], although it should be noted that the data on yellow perch covers a small predator size interval only). The estimation of  $\delta = 0.06$  for Eurasian perch predicts the alternation of cannibal-driven dynamics and dwarfs-and-giants cycles (DG dynamics). With a higher value of  $\delta$ , yellow perch should be closer to or even beyond the boundary of the SC region ( $\delta_1$ ). Although cannibalism is present in yellow perch, the population-dynamic pattern is more reminiscent of SC dynamics than DG dynamics. Thus we conclude that the observed patterns of population dynamics confirm our expectation on the basis of a higher  $\delta$  for yellow perch. More detailed information on  $\delta$  (and  $\varepsilon$ ) of different species would be most useful from the perspective of predicting population dynamics based on these species characteristics.

*Model and data: permanent giants, dynamic giants, or stunting*

By showing that giant cannibals can occur in stable populations, our results complement our previous conclusion that cannibalistic giants can emerge in fluctuation populations (Claessen et al. 2000). In the case of dynamic giants that emerge in fluctuating populations, the mechanism is inherently population dynamical. In the case of permanent giants (e.g., in a stable population) the mechanism relates to the individual capacity

to include 1-yr-old victims. This raises the question of how we can distinguish between these two mechanisms in observed populations with giant cannibals. First, in the case of dynamic giants, giant growth is induced by the breakthrough of an abundant YOY cohort that causes a long-term resource depletion. In the case of permanent giants, induction of giant growth does not correlate to such a population-dynamic event. Second, the emerging population size distributions in the two cases are very different. The dynamic mechanism gives rise to a pronounced bimodal size distribution (or size dimorphism), but the mechanism of permanent piscivores results in a population size distribution that is approximately exponential (cf. Fig. 8e). These different predictions offer opportunities for empirical testing of our model.

In two cases of giants observed in Eurasian perch, the empirical evidence suggest that giants were induced dynamically. In both cases, the appearance of giants was associated with the breakthrough of a dense YOY cohort, which was exploited by a small number of successful cannibals that became giants (LeCren 1992, Claessen et al. 2000, Persson et al. 2000). Moreover, in the period prior to the breakthrough of YOY, giant cannibals were absent. These observations are in concordance with the estimate of  $\varepsilon = 0.45$  for perch, which predicts that giants do not occur in stable populations (since  $\varepsilon < \varepsilon^*$ , the value of  $\varepsilon$  where the population size distribution changes abruptly).

The Arctic char (*Salvelinus alpinus*) is another example of a piscivorous fish species in which giant cannibals are observed in single-species populations (Parker and Johnson 1991, Griffiths 1994, Hammar 2000). In this species, giant cannibals are claimed to occur permanently in stable population size distributions (Parker and Johnson 1991, Johnson 1994) rather than being induced dynamically. Our results show that this hypothesis requires that the upper limit  $\varepsilon$  is sufficiently high that individuals can grow directly from the planktivory niche into the piscivory niche. Considering the estimate of  $\varepsilon \sim 0.47$  based on data from Amundsen (1994), this does not seem very likely at first sight. Two things should be mentioned here. First, species-specific metabolic parameters may tune the effect of  $\varepsilon$ . Future research will show whether char-specific parameters lead to a lower or higher value of  $\varepsilon^*$ . Second, the effect of  $\varepsilon$  relates to the duration of the starvation period between two subsequent passages of YOY through the predation window of cannibals. The starvation period is shortened by reducing the duration of the growing season, under the assumption that starvation is negligible outside the growing season due to low temperatures. Simulations with our model show that on a gradient of the duration of the growing season the population size distribution changes abruptly at a critical season length (D. Claessen, unpublished data), similar to the effect of  $\varepsilon$  (cf. Fig. 7). Populations with permanent piscivory occur at the short-season end of

the simulated gradient and "stunted" populations at the long-season end. We hence cannot rule out the possibility of permanent piscivory even with a relatively low  $\varepsilon$ . It has been claimed that large, cannibalistic Arctic char are common only at high latitudes and high altitudes (Griffiths 1994). The confounding effect of more coexisting species in lakes at lower latitudes and altitudes is a likely explanation of this pattern. Yet the effect of starvation associated with season length can be seen as an alternative hypothesis for this gradient.

Although we can explain the presence of giant cannibals in stable populations, it is hard to explain the claimed bimodal size distribution in stable Arctic char populations with giant cannibals (Parker and Johnson 1991, Johnson 1994, Hammar 2000). Population size distributions that are found beyond the critical upper limit  $\varepsilon^*$  are essentially exponential distributions such as given in Fig. 8e. Required for a bimodal population size distribution is the combination of (1) stagnation of the growth rate near the maximum length in the planktivory niche, and (2) rapid increase of the growth rate beyond this size. This situation can be obtained, for example, by assuming an exclusive food resource for individuals of intermediate size (D. Claessen, unpublished data). Alternatively, an explanation of bimodality may be found by relaxing the assumption that all individuals in a cohort are identical. This allows for other mechanisms such as individual specialization due to flexible behavior, learning, or genetic variation. In future work we hope to explore these mechanisms in a population-dynamic context. Alternatively, we can hypothesize that the bimodal populations are not stable after all. At least in one of the Arctic char lakes with giants and a bimodal size distribution, Lake Korsvatnet in Sweden, there is evidence for cohort dominance (Hammar 1998), which may reflect cohort cycles. However, empirical evidence to show whether or not the induction of giants is associated with the breakthrough of YOY is lacking.

#### ACKNOWLEDGMENTS

We thank Jens Andersson, Jocke Hjelm, Kjell Leonardsson, Sido Mylius, and Lauri Oksanen for interesting and stimulating discussions. The research reported in this article was supported by the Swedish Council for Forestry and Agriculture, the Dutch Science Foundation, and the Swedish Natural Science Research Council. We also thank two anonymous reviewers and the associate editor, whose comments have greatly increased the readability (and decreased the size) of the manuscript.

#### LITERATURE CITED

- Amundsen, P.-A. 1994. Piscivory and cannibalism in Arctic charr. *Journal of Fish Biology* **45**(Suppl. A):181–189.
- Byström, P., and E. García-Berthou. 1999. Density dependent growth and size specific competitive interactions in young fish. *Oikos* **86**:217–232.
- Christensen, B. 1996. Predator foraging capabilities and prey antipredator behaviours: pre- versus postcapture constraints on size-dependent predator-prey interactions. *Oikos* **76**: 368–380.
- Claessen, D., A. M. de Roos, and L. Persson. 2000. Dwarfs

- and giants: cannibalism and competition in size-structured populations. *American Naturalist* **155**:219–237.
- de Roos, A. M. 1997. A gentle introduction to physiologically structured population models. Pages 119–204 in H. Caswell and S. Tuljapurkar, editors. *Structured population models in marine, terrestrial, and freshwater systems*. Chapman and Hall, New York, New York, USA.
- de Roos, A. M., O. Diekmann, and J. A. J. Metz. 1992. Studying the dynamics of structured population models: a versatile technique and its application to *Daphnia*. *American Naturalist* **139**:123–147.
- de Roos, A. M., and L. Persson. 2001. Physiologically structured models—from versatile technique to ecological theory. *Oikos* **94**:51–71.
- Dong, Q., and D. L. DeAngelis. 1998. Consequences of cannibalism and competition for food in a smallmouth bass population: an individual-based modeling study. *Transactions of the American Fisheries Society* **127**:174–191.
- Fagan, W. F., and G. M. Odell. 1996. Size-dependent cannibalism in praying mantids: using biomass flux to model size-structured populations. *American Naturalist* **147**:230–268.
- Fox, L. R. 1975. Cannibalism in natural populations. *Annual Review of Ecology and Systematics* **6**:87–106.
- Griffiths, D. 1994. The size structure of lacustrine arctic charr (Pisces, Salmonidae) populations. *Biological Journal of the Linnean Society* **51**:337–357.
- Gurney, W. S. C., and R. M. Nisbet. 1985. Fluctuation periodicity, generation separation, and the expression of larval competition. *Theoretical Population Biology* **28**:150–180.
- Gurney, W. S. C., and R. M. Nisbet. 1998. *Ecological dynamics*. Oxford University Press, New York, New York, USA.
- Hammar, J. 1998. *Evolutionary ecology of Arctic char (Salvelinus alpinus (L.))*. Dissertation. Uppsala University, Uppsala, Sweden.
- Hammar, J. 2000. Cannibals and parasites: conflicting regulators of bimodality in high latitude arctic char, *Salvelinus alpinus*. *Oikos* **88**:33–47.
- Hirvonen, H., and E. Ranta. 1996. Prey to predator size ratio influences foraging efficiency of larval *Aeshna juncea* dragonflies. *Oecologia* **106**:403–415.
- Hjelm, J., and L. Persson. 2001. Size-dependent attack rate and handling capacity—inter-cohort competition in a zooplanktivorous fish. *Oikos* **95**:520–532.
- Johnson, L. 1994. Long-term experiments on the stability of two fish populations in previously unexploited arctic lakes. *Canadian Journal of Fisheries and Aquatic Sciences* **51**:209–225.
- LeCren, E. D. 1992. Exceptionally big individual perch (*Perca fluviatilis* L.) and their growth. *Journal of Fish Biology* **40**:599–625.
- Lovrich, G. A., and B. Sainte-Marie. 1997. Cannibalism in the snow crab, *Chionoecetes opilio* (O. Fabricius) (Brachyura: Majidae), and its potential importance to recruitment. *Journal of Experimental Marine Biology and Ecology* **211**:225–245.
- Lundvall, D., R. Svanbäck, L. Persson, and P. Byström. 1999. Size-dependent predation in piscivores: interactions between predator foraging and prey avoidance abilities. *Canadian Journal of Fisheries and Aquatic Sciences* **56**:1285–1292.
- Metz, J. A. J., and O. Diekmann, editors. 1986. *The dynamics of physiologically structured populations*. Volume 68 of *Lecture Notes in Biomathematics*. Springer-Verlag, Berlin, Germany.
- Mittelbach, G. G., and L. Persson. 1998. The ontogeny of piscivory and its ecological consequences. *Canadian Journal of Fisheries and Aquatic Sciences* **55**:1454–1465.
- Nilsson, P. A., and C. Brönmark. 2000. Prey vulnerability to a gape-size limited predator: behavioural and morphological impacts on northern pike piscivory. *Oikos* **88**:549–546.
- Orr, B. K., W. W. Murdoch, and J. R. Bence. 1990. Population regulation, convergence, and cannibalism in *Notonecta* (Hemiptera). *Ecology* **71**:68–82.
- Parker, H. H., and L. Johnson. 1991. Population-structure, ecological segregation and reproduction in non-adiabatic arctic charr, *Salvelinus alpinus* (L.), in four unexploited lakes in the Canadian high arctic. *Journal of Fish Biology* **38**(1):123–147.
- Persson, L. 1987. The effects of resource availability and distribution on size class interactions in perch, *Perca fluviatilis*. *Oikos* **48**:148–160.
- Persson, L., K. Leonardsson, A. M. de Roos, M. Gyllenberg, and B. Christensen. 1998. Ontogenetic scaling of foraging rates and the dynamics of a size-structured consumer–resource model. *Theoretical Population Biology* **54**:270–293.
- Persson, L., E. Wahlström, and P. Byström. 2000. Cannibalism and competition in Eurasian perch: population dynamics of an ontogenetic omnivore. *Ecology* **81**:1058–1071.
- Polis, G. A. 1981. The evolution and dynamics of intraspecific predation. *Annual Review of Ecology and Systematics* **12**:225–251.
- Rice, J. A., L. B. Crowder, and E. A. Marschall. 1997. Predation on juvenile fishes: dynamic interactions between size-structured predators and prey. Pages 333–356 in R. C. Chambers and E. A. Trippel, editors. *Early life history and recruitment in fish populations*. Chapman and Hall, London, UK.
- Sanderson, B. L., T. R. Hrabik, J. J. Magnuson, and D. M. Post. 1999. Cyclic dynamics of a yellow perch (*Perca flavescens*) population in an oligotrophic lake: evidence for the role of intraspecific interactions. *Canadian Journal of Fisheries and Aquatic Sciences* **56**:1534–1542.
- Shine, R. 1991. Why do larger snakes eat larger prey items? *Functional Ecology* **5**:493–502.
- Sousa, W. P. 1993. Size-dependent predation on the salt-marsh snail *Cerithidea californica* Haldeman. *Journal of Experimental Marine Biology and Ecology* **166**:19–37.
- Tripet, F., and N. Perrin. 1994. Size-dependent predation by *Dugesia lugubris* (Turbellaria) on *Physa acuta* (Gastropoda)—experiments and model. *Functional Ecology* **8**:458–463.
- Wahlström, E., L. Persson, S. Diehl, and P. Byström. 2000. Size-dependent foraging efficiency, cannibalism and zooplankton community structure. *Oecologia* **123**:138–148.
- Werner, E. E. 1974. The fish size, prey size, handling time relation in several sunfishes and some implications. *Journal of the Fisheries Research Board of Canada* **31**:1531–1536.
- Werner, E. E., and J. F. Gilliam. 1984. The ontogenetic niche and species interactions in size-structured populations. *Annual Review of Ecology and Systematics* **15**:393–425.
- Wilbur, H. M. 1988. Interactions between growing predators and growing prey. Pages 203–218 in B. Ebenman and L. Persson, editors. *Size-structured populations: ecology and evolution*. Springer-Verlag, Berlin, Germany.